15th Triennial World Congress, Barcelona, Spain

ACTIVE SUPERSONIC FLOW CONTROL USING HYSTERESIS COMPENSATION AND ERROR GOVERNOR[1]

Marina Tharayil, Andrew Alleyne

University of Illinois at Urbana-Champaign
Department of Mechanical and Industrial Engineering
1206 West Green Street
(217) 244-6534 (fax), alleyne@uiuc.edu

Abstract: This paper introduces a novel concept termed Smart Mesoflaps for Aeroelastic Recirculation Transpiration (SMART) for controlling shock/boundary-layer interactions (SBLI) in supersonic jet inlets. The control strategy for a subsystem of the SMART project, subject to hysteresis and actuator saturation, is presented. A Hysteresis Compensation scheme, as well as results from experimental application of HC to the SMART system are presented next. A generalized error governing scheme for PID controllers to compensate for actuator saturations is also developed. Finally, the PID with HC and the error governing method is experimentally applied to a benchtop SMART subsystem and is shown to be successful at preventing excessive control efforts. *Copyright © 2002 IFAC*

Keywords: Actuators, Control design, Saturation, PID controllers, Error analysis, Error control, Aerospace control, Flow control, Hysteresis.

1. MOTIVATION

The work presented in the paper was motivated by actuator limitations in the SMART Project. Smart Mesoflaps for Aeroeastic Recirculation Transpiration (SMART) is a DARPA funded project at the University of Illinois aimed at rendering mass and momentum transfer for controlling shock/boundary-layer interactions (SBLI) in supersonic jet inlets. The SMART system takes advantage of the pressure differential that arises between the areas upstream and downstream of the shock in a supersonic jet inlet. It consists of a matrix of mesoflaps covering an enclosed cavity. The flaps locally deflect in a cantilever mode due to the aerodynamic pressure distribution on them to achieve appropriately angled bleed and injection. Overall SMART system, under passive aeroelastic transpiration, is described in detail in (Crisman, 1999; Wood, et. al.,1999).

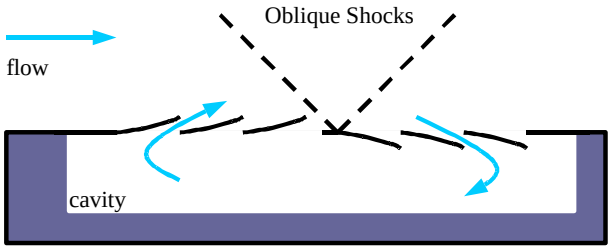

Fig. 1. Schematic of the SMART concept.

A schematic of the SMART system is shown in the figure 1. Although positive system performance is achieved using this system, the 'smart' part of the SMART is utilized to control the flap deflection to optimize the amount of recirculation (and thus the performance). This Thermally-Activated Smart Material (TASM) design uses NiTi shape memory alloy (SMA) as an actuator for the flaps to control the amount of recirculation. A detailed explanation of the properties of nitinol can be found in (Shaw,

[1] This work is supported by DARPA under contract F49620-98-1-0490

1995). The property of interest in this project is that NiTi consists of two (or more) phases with different mechanical properties and can transform from one phase to the other. This transformation can be induced either mechanically or thermally. Consequently, by controlling the temperature of the material, one can control the composition of the NiTi. In current SMART design the mesoflap material is flat annealed, so that when heated it will experience an increase in stiffness, and as a result attempt to revert to a closed position. This closed position is not reached because of the pressure differential, but due to the change in Young's modulus, E, between the Martensite and Austenite phase, the amount of flap deflection can be varied within boundaries defined by the applied pressure differential and the minimum and maximum values of E. In this investigation, a single layer of nitinol is used, with an external heat source providing power input to drive the phase transformations. The stiffness of the material, E, (and therefore the amount of deflection) is thus controlled. The subsystem modeling of a single flap has been presented in (Tharayil and Alleyne, 2001). The work presented in the paper is focused on closed loop control of a single mesoflap under realistic flow conditions.

2. EXPERIMENTAL SYSTEM DESCRIPTION

In the initial stages of TASM design, a bench-top test has been done to control the deflection of one nitinol flap under loading similar to the pressure difference across a flap in actual use. A single flap case was chosen as the control experiment because it is the simplest case and will provide an understanding of nitinol behavior under pressure loading and with applied temperature. The current experimental set-up consists of a pressure chamber with a rectangular opening and is supplied with high pressure air. The flap, 60mm x 15mm x 1.524E^{-4}mm in dimension, sits over this opening, and is held in place by a frame and epoxy. A specialized miniature resistance heater is attached to the inner surface of the flap to provide the thermal energy required for the material transformation. A laser displacement sensor is mounted above the flap to measure the deflection of the flap. The chamber is equipped with four pressure taps and a pressure transducer to measure the pressure inside the chamber. A schematic drawing of the system is given in figure 2.

The block diagram shown in figure 3 depicts the major components in this system. The controller uses the error, e, to calculate a voltage command to be sent to the amplifier, which results in a proportional amount of current being sent to the heater. The heater converts the electrical energy into thermal energy, thereby inducing the nitinol transformation. The NiTi transformation results in a change of stiffness, leading to a change in the deflection. Block 3 in figure 3 models the nitinol response to power input.

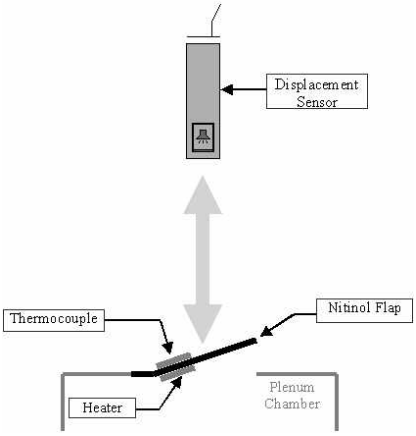

Fig. 2. A schematic of the experimental set-up.

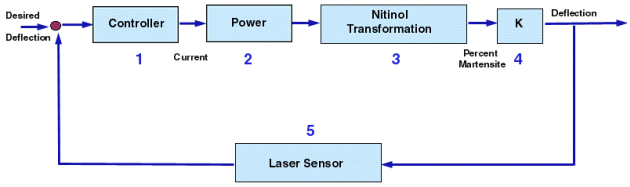

Fig. 3. Block diagram of the control strategy

As was mentioned previously, Shape Memory Alloys (SMAs) undergo transition between martensite and austenite phases as the temperature is varied. This transformation begins when the SMA is brought to the austenite start temperature (A_s), and will be complete as the SMA reaches the austenite finish temperature (A_f). Similarly, austenite to martensite transformation occurs as the temperature goes from the martensite start temperature (M_s) to the martensite finish temperature (M_f). Since the forward and reverse transformations do not occur at the same temperatures, SMAs exhibit significant hysteresis. Figure 4 shows the Temperature-Young's Modulus relation of the nitinol used in the SMART project, obtained from experiments conducted at the Materials Testing Laboratory of the University of Illinois. The representation of the hysteresis can be modeled quite well using a Preisach Model, as presented in (Gorbet and Morris, 2001; Majima, et. Al., 2001). A simpler model is used in the SMART project, the details of which are given in (Tharayil & Alleyne, 2001). This hysteresis, which manifests itself in the system response as a delay when the reference changes directions, led to the compensation scheme presented in the paper.

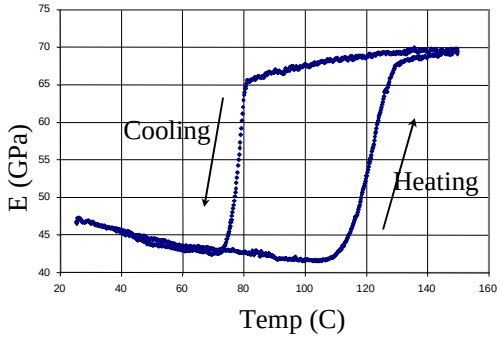

Fig. 4. Temperature-Stiffness(E) Characteristics of Nitinol used at UIUC.

A Proportional-Integral-Derivative (PID) controller was chosen for the SMART project because of its simplicity and effectiveness. The control signal, *u*, is given by:

$$u = K_p e + K_i \int e + K_d (de/dt) \qquad (1)$$

During the initial tuning of the controller, gains K_p, K_i, and K_d of 0.5, 0.1, and 0.5 respectively were chosen because they resulted in a stable and acceptably fast response. System response to a step reference is studied here. The control effort generated using the PID controller is of large magnitude for a period after the step in the deflection reference command. This results in large currents being sent to the heater, which in turn leads to heater burn-outs due to exceeding the power ratings of the heater. This motivated the investigation into ways to prevent large control signals.

3. HYSTERESIS COMPENSATION (HC) SCHEME

This scheme was implemented to avoid the delay in response caused by the hysteretic nature of the actuator. In other words, the linear controllers used thus far assume a linear relation between control input and system response. This is a valid approximation as long as the control direction is constant. Once the control effort changes direction (increasing to decreasing), there is a pause in the nitinol response because of the disparity between the Temperature-increase and Temperature-decrease curves shown in figure 5. The basic idea of the hysteresis compensation is to reduce this gap in deflection response time by applying a discontinuity in the control input. In other words, for error > 0 (stiffness increasing), $u = u + u_{step}$. For symmetry, and to operate in the center of the hysteresis, one would apply $u = u - u_{step}$ for error < 0, but this would result in negative current in our case. This is not an option in the SMART experiment because only one-way actuation is available here.

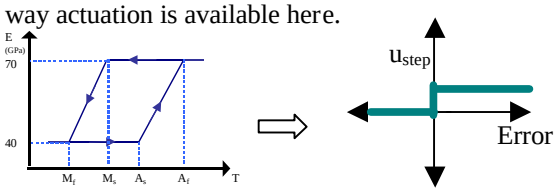

Fig. 5. (b) step change in control effort to compensate for material hysteresis (a).

However, in a real system, the above scheme results in oscillations about the set point, due to noise in the signal and the slow response of the material. When the error is small, close to zero, noise in the signal causes the HC to step up and down rapidly, resulting in oscillations about the set point. Therefore, a backlash (BL) scheme was added to the error signal to prevent the occurrence of such oscillations. Adding this deadband to the error signal allows for small deviations of the error signal about zero without large changes in the control signal. In this way, one can improve the response of hysteretic actuators. Figure 6 shows the effect of adding the backlash block to the HC step and figure 7 displays the advantage of using HC along with the original PID controller with gains 0.5, 0.1, and 0.5 respectively. Part (a) shows the deflection response using various values of HC increments and compares them to the baseline case with no HC. Here HC is the value of the increment in control effort to compensate for the material hysteresis. Increments of 0.1 and 0.15 Amps were used, and best results were given by the higher increment. A backlash of 0.1 was added to both cases. Part (b) shows the control efforts generated for the different cases.

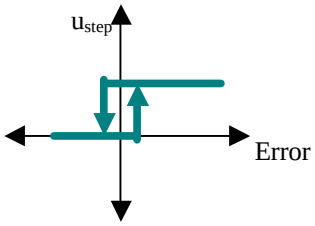

Fig. 6. HC with a dead band added to error.

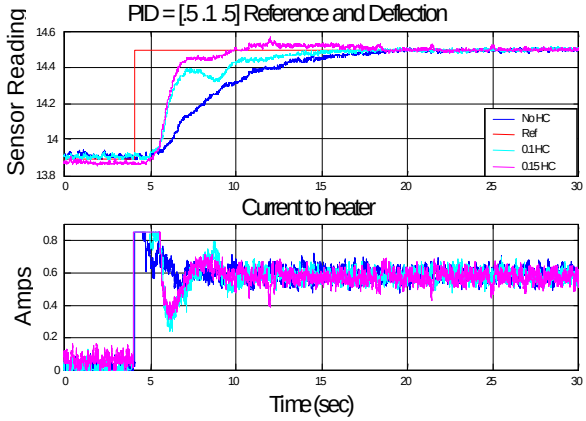

Fig. 7. Results from a PID controller using HC

4. ERROR GOVERNOR (EG)

Actuator saturation, similar to what is observed in SMART, is a common non-linearity in practical control systems. One solution to this problem in the SMART system is to limit the output sent to the amplifier. This method will eliminate the heater burn out problem, but it could lead to a phenomenon called integrator wind-up. Integrator wind up occurs when a system has actuator saturation and an integrator in its controller. A detailed description of integrator wind up can be found in (Franklin, et. al., 1994). Some form of anti-windup mechanism must be implemented in the PID controller to achieve good system performance. An overview of available anti-wind up strategies is presented next.

The Variable Limit PI-Controller was developed by (Safaric, et. al., 1991) for systems with plant input saturation that use PI-controllers. A variable limit is introduced in the integral branch of the controller to ensure that the control effort does not exceed the saturation limit. The next four control strategies are designed for a system with plant input saturation that

use PID controllers. A detailed account of the following four anti-windup strategies can be found in (Bohn, et. al., 1995). In the Conditional Integrator method, the integration is switched on or off depending on certain conditions. In the Limited Integrator method, a feedback signal is created from the integrator output by feeding the integrator output through a dead zone with a high gain. The dead zone is used to reduce the integrator input. In the "classical" anti-windup method called Tracking Anti-Windup, once the controller output exceeds the actuator limits, a feedback signal is generated from the difference of the saturated and unsaturated control signals and used to reduce the integrator output. In this design, a very high initial controller output (due to the P and D terms) will give a large feedback signal to the integrator. The Modified Tracking Anti-Windup method avoids this slow response by introducing an additional limit on the proportional-derivative part of the control signal used to generate the anti-windup-feedback signal. All the above anti-windup schemes assume that the saturation is a result of the integral term, and apply corrective actions to the integral terms. The error governor, presented next, addresses the integrator windup problem without making that assumption

The idea behind the error governor is to design a linear control loop ignoring the saturations and then to introduce a supervisor loop. The system operates linearly as designed when the references (or disturbances) are small; for signals large enough to cause saturations, the control law is modified to ensure stability and to preserve the transient behavior of the linear system. Such a control scheme reduces/eliminates the following two major limitations caused by saturation: (1) for multivariable systems, control saturations alter the direction of the control vector, and (2) for a linear compensator with integrators, the occurrence of reset-windup results due to the continuous integration of error during actuator saturation. This idea of the generalized error governor presented here was previously introduced in (Kapasouris, et. al., 1988).

To start with, a few definitions and observations are stated in order to introduce the notion of the Error Governor. For a system given by

$$\begin{aligned} \dot{x}(t) &= Ax(t) \\ y(t) &= Cx(t) \end{aligned} \quad \text{with } x(0) = x_0, \qquad (2)$$

the solution can be written as $y(x_0,t) = Ce^{At}x_0$. A scalar-valued function g(x) is defined as follows:

$$g(x_0): \Re^n \to \Re^1,\ g(x_0) = \left\| y(x_0,t) \right\|_\infty \qquad (3)$$

It can be shown that g(x) is finite if the system described in Equation (3) is neutrally stable. Now we define a set $B_{A,C}$ as the set of all $x \in \Re^n$ with $0 \le g(x) \le 1$. This is a set of all states such that the scalar function (the infinity norm of y(t)) remains between 0 and 1.

$$B_{A,C} = \{0 \le g(x) \le 1\} \qquad (4)$$

From this definition, we see that if the system (2) has an initial condition $x_0 \in B_{A,C,}$ the output of the system, y(t), will satisfy $\left\| y(t) \right\|_\infty \le 1$. Consider the system given below.

$$\begin{aligned} \dot{x}(t) &= Ax(t) + Bu(t) \\ y(t) &= Cx(t) \end{aligned} \qquad (5)$$

If the system is neutrally stable and B=0, then $g(x) < \infty\ \forall x \in \Re^n$. The goal now is to keep the output of the linear system (6) bounded ($|y(t)| \le 1,\ \forall t$) for any input u(t). This can be done using a time-varying scalar gain as follows:

$$\begin{aligned} \dot{x}(t) &= Ax(t) + Bl(t)u(t) \\ y(t) &= Cx(t) \end{aligned} \qquad (6)$$

The value of $\lambda(t)$ ranges from 0 to 1 and can be modified such that the output remains within the bounds. Now the basic problem becomes finding the maximum gain $\lambda(t_0)$, $0 \le \lambda(t_0) \le 1$, such that for all u(t), $t > t_0$, $\exists\ \lambda(t)$, $t > t_0$, such that the output satisfies, $|y_i| \le 1$, for all *i*, $t > t_0$.

Consider a multivariable closed loop system consisting of a plant, a compensator, and saturation at the plant input. Here, the compensator can be thought of as an independent linear system, as shown in figure 8, with input e(t) and output u(t), and can be represented by Equation 7,

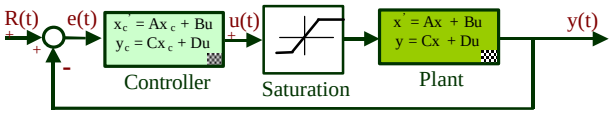

Fig. 8. Schematic of plant and controller

$$\begin{aligned} \dot{x}_c(t) &= A_c x_c(t) + B_c e(t) \\ u(t) &= C_c x_c(t) \end{aligned} \qquad (7)$$

where error e(t) = r(t) – y(t). The error governor modifies the error e(t) to $e_\lambda(t)$ only when the references are large enough to cause the controls to saturate. The modified compensator equations are given below.

$$\begin{aligned} \dot{x}_c(t) &= A_c x_c(t) + B_c\, l(t) e(t) \\ u(t) &= C_c x_c(t) \\ \dot{u}(t) &= C_c A_c x_c(t) + C_c B_c\, l(t) e(t) \\ \text{where } & e_l(t) = l(t) e(t) \end{aligned} \qquad (8)$$

Here, $\lambda(t) = 1$ for small enough errors, and for large errors, $\lambda(t)$ will take values to modify the error and prevent the controls from exceeding their limits. This is done by defining a function g(x) and a set $B_{A,C}$ and by constructing $\lambda(t)$ such that the states of

the compensator remain in $B_{A,C}$ for any reference. Define g(x) and $B_{A,C}$ as follows.

$$g(x_0):\ g(x_0) = \|u(t)\|_\infty \qquad (9)$$

Where

$$\dot{x}_c(t) = A_c x_c(t); x_c(0) = x_0$$
$$u(t) = C_c x_c(t) \qquad (10)$$

$$B_{A,C} = \{x : g(x) \le 1\} \qquad (11)$$

For every time t, choose λ(t) such that:

- if $x_c(t) \in \text{Int}\{B_{A,C}\}$, then λ(t) = 1
- if $x_c(t) \in \text{Bd}\{B_{A,C}\}$, then choose largest λ(t) such that:

$$\lim_{e \to 0} \sup \frac{g(x_c(t) + e[A_c x_c(t) + B_c l(t) e(t)]) - g(x_c(t))}{e} \le 0 \qquad (12)$$

- if $x_c(t) \notin \text{Int}\{B_{A,C}\}$, then choose λ(t) to minimize (12).

It has been proven by [Kapasouris, et. al.,1988] that if at time t = 0 the compensator states belong in the set $B_{A,C}$, then the EG operator defined as λ(t) exists and the signal u(t) remains bounded for any signal e(t).

5. EG APPLIED TO PID CONTROLLERS

For a PID controller, the control equation equivalent to (7) can be written as follows:

$$u = k_d \dot{e} + k_p e + k_i \int e \qquad (13)$$

Next, $B_{A,C}$ in the previous subsection was defined as the set of all controller states such that the output, u, remains within the saturation boundaries. For the PID controller, the controller states are given by the error and the integral of the error. The conditions for selecting λ(t) presented above can be tailored to the PID case as follows:

- If (e, ∫e) are such that $u(e, \int e) < u_{sat}$, then λ(t) = 1.
- If (e, ∫e) are such that $u(e, \int e) = u_{sat}$, then choose λ(t): $\dot{u}$ (e, ∫e) = 0.
- If (e, ∫e) are such that $u(e, \int e) > u_{sat}$, then choose λ(t) to minimize $\dot{u}$ (e, ∫e).

In other words, modify the error such that du/dt ≤ 0 when u reaches its saturation limits.

Now, let us consider the control effort and its derivative. Assuming that the control effort at time t = 0 is within the actuator saturation limits, for the second condition, one would set the derivative $\dot{u}$ to equal zero.

$$u = k_d \dot{e} + k_p e + k_i \int e$$
$$\dot{u} = k_d \ddot{e} + k_p \dot{e} + k_i e = 0 \qquad (14)$$

The second equation in (14) is a second order differential equation, whose solution can be written as:

$e = Ae^{\alpha t}$ where $a_{1,2} = -\frac{k_p}{2k_d} \pm \sqrt{\left(\frac{k_p}{2k_d}\right)^2 - \frac{k_i}{k_d}}$ (15)

This leads to solutions:

$$e_l(t) = Ae^{\left\{-\frac{k_p}{2k_d} + \sqrt{\left(\frac{k_p}{2k_d}\right)^2 - \frac{k_i}{k_d}}\right\}t} + Be^{\left\{-\frac{k_p}{2k_d} - \sqrt{\left(\frac{k_p}{2k_d}\right)^2 - \frac{k_i}{k_d}}\right\}t} \qquad (16)$$

or $e_l(t) = e^{-\frac{k_p}{2k_d}t}\{C\sin(w_d t) + D\cos(w_d t)\}$;

where $w_d = \sqrt{-\left(\frac{k_p}{2k_d}\right)^2 + \frac{k_i}{k_d}}$

depending on the sign of the term inside the square root. The coefficients, A, B, C and D in the above equations depend on the initial conditions. The initial conditions should be chosen such that at the time of switch, $t_s, e_l(t_s) = e(t_s)$, and the derivative is such that $u(e_\lambda, \int e_\lambda) = u_{sat}$. Therefore, the EG can be applied to the PID as follows: If $u < u_{sat}$, $e = e_{actual}$; else, $e = e_\lambda(t)$. This ensures that as long as $u(0) < u_{sat}$, the controller will not saturate. However, due to the discontinuities in the error signal, as it switches from e to e_λ or vice versa, the control effort should be frozen for one time step when the transfer of e takes place.

6. GENERALIZED MODIFIED EG IN SMART

For the SMART controller with the PID gains [.5 .1 .5], the error $e_\lambda(t) = Ae^{\alpha t}$ which generates $u(e, \int e) = u_{sat}$ is given by:

$$e_l(t) = Ae^{\left\{-\frac{k_p}{2k_d} + \sqrt{\left(\frac{k_p}{2k_d}\right)^2 - \frac{k_i}{k_d}}\right\}t} + Be^{\left\{-\frac{k_p}{2k_d} - \sqrt{\left(\frac{k_p}{2k_d}\right)^2 - \frac{k_i}{k_d}}\right\}t} \qquad (17)$$

where $\alpha_{1,2} = -0.5 \pm 0.2236 = -0.7236, -0.2764$ and A = -B = 1.05. The error governor was implemented on this controller in coordination with HC = 0.15. A saturation value of 0.85 Amps was chosen since currents higher than 0.9 Amps result in heater burnout. Results can be seen from figure 9. Part (a) in the Figure 9 shows the reference and actual deflection of the mesoflap. Part (b) shows the currents u_{actual} and u_{model} generated by the controller. Part (c) shows the actual and modified errors. Notice that there is an upsurge in the control effort as the modified error switches from the generated error to the actual error. This is caused by a large derivative term which arises as a result of the discontinuity in the error signal, as explained in the previous section. This instantaneously large u arises because u_{model} does not predict the derivative that results from the switch. In order to avoid such spikes in u, the derivative term has been modified as follows:

if $\left|\frac{de}{dt}\right|$ > set limit, then $\left|\frac{de}{dt}\right| = \left|\frac{d(e(t-\Delta t)}{dt}\right|$, e = e(t-Δt). (18)

Here Δt is of the order of the sampling time at which the controller is being implemented. In other words, when there are discontinuities in the error signal, set the derivative and proportional term to equal their values from the previous time step to avoid the large derivative caused by the discontinuity. From the time step after the occurrence of the switch, the derivative and proportional terms will use the actual signals, and thus remain within bounds. Figure 10 shows results using this approach. One can see that the error governor is effective in limiting the control effort within the saturation limits.

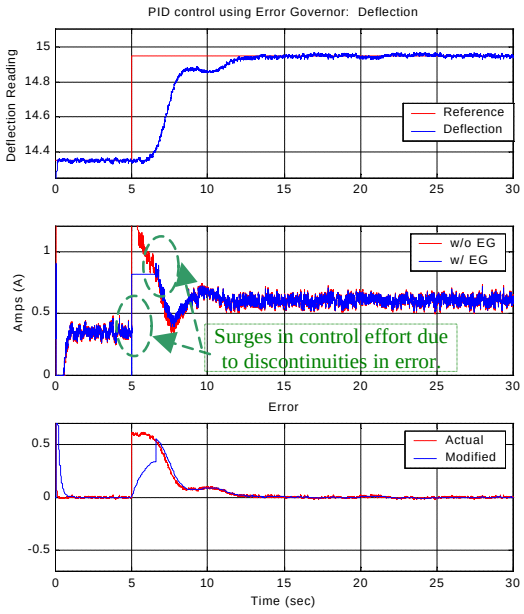

Fig. 9. Results using a PID controller with EG.

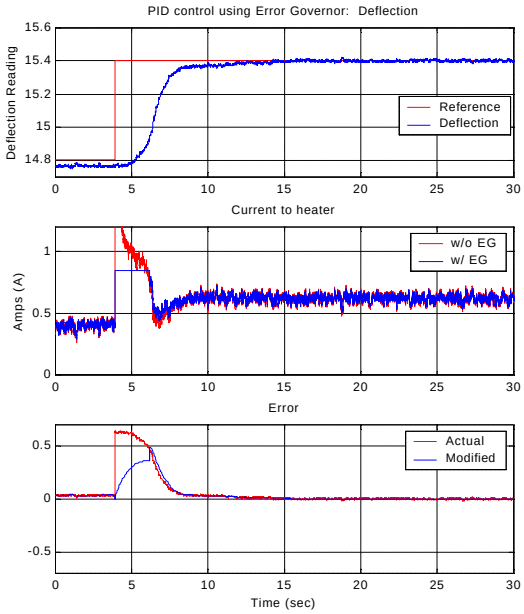

Fig. 10. Results using the EG with controlled derivative and proportional terms.

7. CONCLUSIONS

The control method for a plant with hysteresis and saturation is presented. A simple PID controller has been augmented using Hysteresis Compensator and Error Governor. A generalized method for saturation compensation for PID controllers has been developed. This controller modifies the error sent to the PID controller in order to avoid saturation. This method is independent of the plant (as long as it is open-loop marginally stable); thus it can be used for any PID controlled system to avoid saturation. Experimental verification of the effectiveness of HC and EG has been realized on the SMART system.

REFERENCES

Bohn, C., Atherton, D. P. (1995). "An Analysis Package Comparing PID Anti-Windup Strategies", *IEEE Control Systems Magazine* , **15** Issue 2, April, pp 34 – 40

Crisman, P. C. (1999). "*Modeling, Analysis, Simulation, and Control of a Smart Flap Actuator For a Shock Boundary Layer Interaction Control System*", M.S. Thesis, Dept. of M&IE, Univ. of Illinois at Urbana-Champaign.

Franklin, G. F., Powell, D. J., Emami-Naeini A. (1994). Feedback Control of Dynamic Systems, pp. 196-200. Addison-Wesley Publishing Company, Inc.,

Gorbet, R, Morris, K, (2001). "Passivity-Based Stability and Control of Hysteresis in Smart Actuators", *IEEE Transactions on Control Systems Technology*, **9**, No. 1, pp. 5-16.

Kapasouris, P., Athans, M., Stein, G. (1988), "Design of Feedback Control Systems for Stable Plants with Saturating Actuators", *Proceedings of the 27th IEEE Conference on Decision and Control*, Austin, TX, pp. 469-479.

Majima, S., Kodama, K., Hasegawa, T., (2001). "Modeling of Shape Memory Alloy Actuator and Tracking Control System with the Model", *IEEE Transactions on Control Systems Technology*, **9**, No. 1, pp. 54-59.

Safaric, P., Jazernic, K., Borojevic, D. (1991). "PI controller for Avoiding Integrator Wind-up in Systems with Plant Input Saturation", *Proceedings of IEEE 6th Electrotechnical Conference*, Mediterranean , **2**, pp. 803 – 806.

Shaw, A., Kyriakides, S. (1995). "Thermomechanical Aspects of NiTi", *Journal of the Mechanics and Physics of Solids*, **43**, No. 8, pp. 1243-1280

Wood, B., Loth, E., and Geubelle, P. H. (1999). "Mesoflaps for Aeroelastic Transpiration for SBLI Control", *37th Aerospace Science Meeting*, Reno NV, AIAA 99-0614